Hindawi Publishing Corporation
Journal of Nanomaterials
Volume 2013, Article ID 868540, 6 pages
http://dx.doi.org/10.1155/2013/868540

Research Article

Effect of Mechanical Deformation on Thermoelectric Properties of p-Type $(Bi_{0.225}Sb_{0.775})_2Te_3$ Alloys

Sung-Jin Jung,[1,2] Seong Keun Kim,[1] Hyung-Ho Park,[2] Dow-Bin Hyun,[1] Seung-Hyub Baek,[1,3] and Jin-Sang Kim[1]

[1] *Future Convergence Research division, Korea Institute of Science and Technology, Seoul 136-791, Republic of Korea*
[2] *Department of Material Engineering, Yonsei University, Seoul 120-749, Republic of Korea*
[3] *Department of Nanomaterials Science and Technology, University of Science and Technology, Daejeon 305-333, Republic of Korea*

Correspondence should be addressed to Seung-Hyub Baek; shbaek77@kist.re.kr and Jin-Sang Kim; jskim@kist.re.kr

Received 13 June 2013; Revised 11 September 2013; Accepted 13 September 2013

Academic Editor: Chan Park

The effect of mechanical deformation and annealing on thermoelectric properties of p-type $(Bi_{0.225}Sb_{0.775})Te_3$ was performed. The ingots were prepared by melting, followed by quenching method using source materials with compositions of $(Bi_{0.225}Sb_{0.775})_2Te_3$. Rectangular shaped specimens ($5\times5\times12$ mm^3) were cut from ingots and then cold-pressed at 700 MPa for 2 to 20 times by changing the press direction perpendicular to previous one. The cold-pressed samples have been annealed in a quartz ampoule at 573 K. The grain size of the samples was controlled by the number of cold-pressing process and annealing time. Fine grain structure with a grain size of not more than 10 μm is obtained in highly deformed samples. The Seebeck coefficient of the deformed samples were gradually increased with annealing and converged to the similar value of about 225 μV/K after 30 hrs. The small grain size in highly deformed sample enables a rapid increase of Seebeck coefficient with annealing time (~2 hrs.), indicating that the thermal energy needed to recrystallize in highly deformed specimens is lower than that in low deformed specimens. Z values are rapidly increased with annealing time especially in highly deformed alloys, and converge to about 3.0×10^{-3}/K at room temperature. A higher thermoelectric performance could be expected by the optimization of composition and microstructural adjustment. The present study experimentally demonstrates a simple and cost-effective method for fabricating Bi-Te-based alloys with higher thermoelectric performance.

1. Introduction

Bi_2Te_3-related compounds such as solid solutions of Bi_2Te_3 and Sb_2Te_3 have been widely studied over the past decades due to their excellent properties for use in thermoelectric cooling and power generation near the room temperature [1–3]. Currently, one stream of thermoelectric researches follows the improving thermoelectric dimensionless Figure-of-Merit ($ZT = \alpha^2\sigma T/\kappa$, where α, σ, κ, and T are the Seebeck coefficient, electrical conductivity, thermal conductivity, and absolute temperature) by fabricating nanostructures with existing thermoelectric (TE) materials [4–6]. Thermoelectric nanostructures can be produced by many techniques, such as hydrothermal methods [7], wet chemical reactions [8], and ball milling [2, 4]. Conventional ball milling has been employed to produce large quantities of fine particles with a size of one to several microns and this process can be readily scaled up for commercial use at reasonable cost. In order to obtain TE materials, the TE particles should be consolidated into a dense solid using various methods, such as spark plasma sintering [5, 9], hot-pressing [2, 4, 7, 10], and extrusion methods [11, 12].

Generally cold-pressing only mechanically compacts the particles and thus the density of cold-pressed composites tend to be low, resulting in a material with poor mechanical and thermoelectric properties. To improve the mechanical and electrical properties of the composites, the cold-pressing should be followed by sintering at appropriated temperatures. Thus, the techniques used to produce TE nanocomposites can be any combination of a powder preparation method and a composited consolidation methods. As a powder preparation method, high energy ball milling is generally used with source materials of crystalline Bi-Sb-Te alloy ingots which are prepared by zone melting and Bridgman methods [5, 9, 11, 13].

In this paper, we introduce a simple fabrication method of randomly oriented polycrystalline Bi-Sb-Te based alloys which is not employing conventional powdering process. $(Bi_{0.225}Sb_{0.775})_2Te_3$ compound was prepared by melting the source elements followed by serial processing with cold-pressing process and recovery annealing. The effects of degree of deformation and annealing time on the thermoelectric properties were investigated. Thermoelectric properties are discussed on the point of view of microstructural evolution of cold-pressed sample with annealing.

2. Experimental Procedures

Elemental bismuth (Bi), antimony (Sb), and tellurium (Te), with purity of 99.99% were used as starting materials for synthesis of $(Bi_{0.225}Sb_{0.775})_2Te_3$ compounds. Each of three materials was weighed according to the chemical formula of $(Bi_{0.225}Sb_{0.775})_2Te_3$, loaded into quartz ampoules, and sealed under a vacuum of 10^{-6} Torr. Before loading the mixture, the quartz ampoule, whose inner diameter was 11 mm, was chemically etched with 10% HF + 90% HNO_3 and then washed with deionized water to remove any surface impurities. Bi, Sb, and Te were melted and rocked at 1023 K for 4 hrs and then rapidly cooled to room temperature. The cylindrical ingots were then cut into bar-shaped specimen ($5 \times 5 \times 12\,mm^3$) for the measurement of thermoelectric properties and cold-pressing. Cold-pressing was performed by applying the mechanical pressure of 700 MPa using tool-steel die. The press direction was perpendicular to the 5 mm × 5 mm plane of the specimen. After the first pressing step, the specimen was removed from the press die and pressed again with the press direction perpendicular to newly formed 5 mm × 5 mm face of deformed specimen. These cold-press steps were carried out for 2 to 20 times to change the amount of mechanical deformation and then annealed at 573 K up to 30 hrs.

X-ray diffraction patterns of quenched ingot, compacted pallets after pressing and annealing process were obtained using a BRUKER D8 diffractometer. Specimen density was calculated from precise measurements of the specimen's dimension and mass. The electrical resistivity (ρ) was measured by the conventional AC four-probe method. The Seebeck coefficient was measured by a method based on the slope of a voltage versus temperature-difference curve. The thermoelectric properties of the same samples were also measured by using commercial equipment (ZEM-2M, Ulvac Inc.) and two sets of measurements are within ±1% of each other. Microstructural analysis was carried out using a scanning electron microscope (Hitachi S-4300) equipped with an Electron Back-Scatter Diffraction (EBSD, Bruker e-Flash) system. The Figure-of-Merit (Z) was determined by the Harman method in vacuum chamber (10^{-5} Torr). Four Pt-wires with 40 μm in diameter were bonded to both ends of rectangular-shaped sample, two for current flow and the other two for voltage measurement.

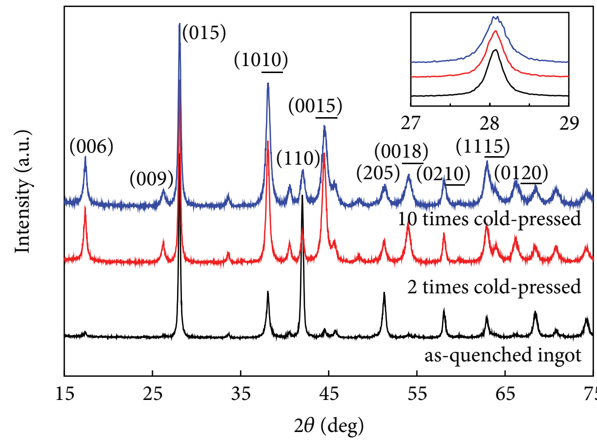

FIGURE 1: X-ray diffraction patterns of as-quenched ingot and $(Bi_{0.225}Sb_{0.775})_2Te_3$ alloys with different number of cold pressing.

3. Results and Discussion

Figure 1 shows the X-ray diffraction patterns of the as-quenched $(Bi_{0.225}Sb_{0.775})_2Te_3$ ingot and cold-pressed pallets on the surface perpendicular to the press direction. The peak intensities were normalized by (015) diffraction peaks of the samples. All diffraction peaks were assigned to a rhombohedral Bi_2Te_3-Sb_2Te_3 structure. The presence of strong diffraction peaks in the cold-pressed samples such as (006), (009), (00$\underline{15}$), and (00$\underline{18}$) indicates the alignment of grains along the $[00\ell]$ direction, that is, reorientation of the *ab* planes of the grains took place during the repressing process even at room temperature. Inset of Figure 1 is magnified (015) diffraction peak. The more re-pressing process, the more broadened the peaks are in the patterns suggest that fine grain-sized particles are formed and/or complicated natures of the residual stress and strain remain in pallets.

Figure 2 shows the X-ray diffraction patterns of cold-pressed samples taken perpendicular to the direction of press with different annealing times. Solid dots in the figure are the positions of peak heights with standard intensities of powder patterns for rhombohedral $(Bi_{0.2}Sb_{0.8})_2Te_3$ phases (JCPDS number 72-1836). In 10 times cold-pressed and 30 hrs annealed sample, the peaks position and intensities exhibited almost the same as that of standard powder patterns, which indicates that the *ab* oriented grains which are aligned perpendicular to press direction in cold-pressed specimen were randomly rearranged by recrystallization during the annealing process. It was also noted that the diffraction peaks of the annealed samples were narrowed with the increase of annealing time (shown in the inset of Figures 2(a) and 2(b)), supporting that the grain growth took placed during the heat treatment.

To obtain detailed information on the microstructures, especially the grain-boundary characteristics, Electron Back-Scatter Diffraction (EBSD) analysis according to the number

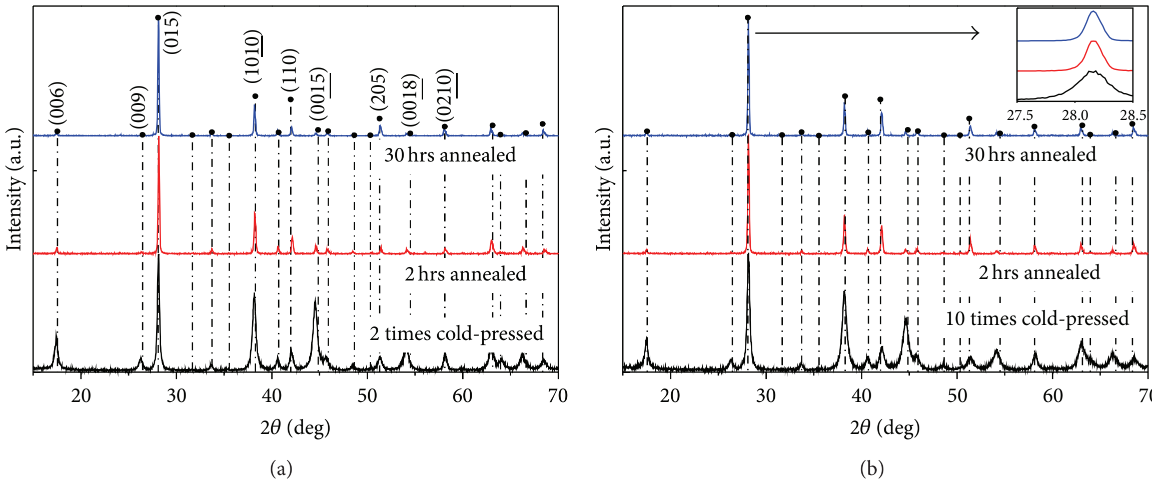

Figure 2: X-ray diffraction patterns of $(Bi_{0.225}Sb_{0.775})_2Te_3$ versus annealing time at 573 K for (a) 2 times cold-pressed, and (b) 10 times cold-pressed samples. Solid dots represent the position of peak heights from standard powder pattern (JCPDS # 72-1836). Inset in (b) indicates magnified (0015) diffraction peaks of the samples.

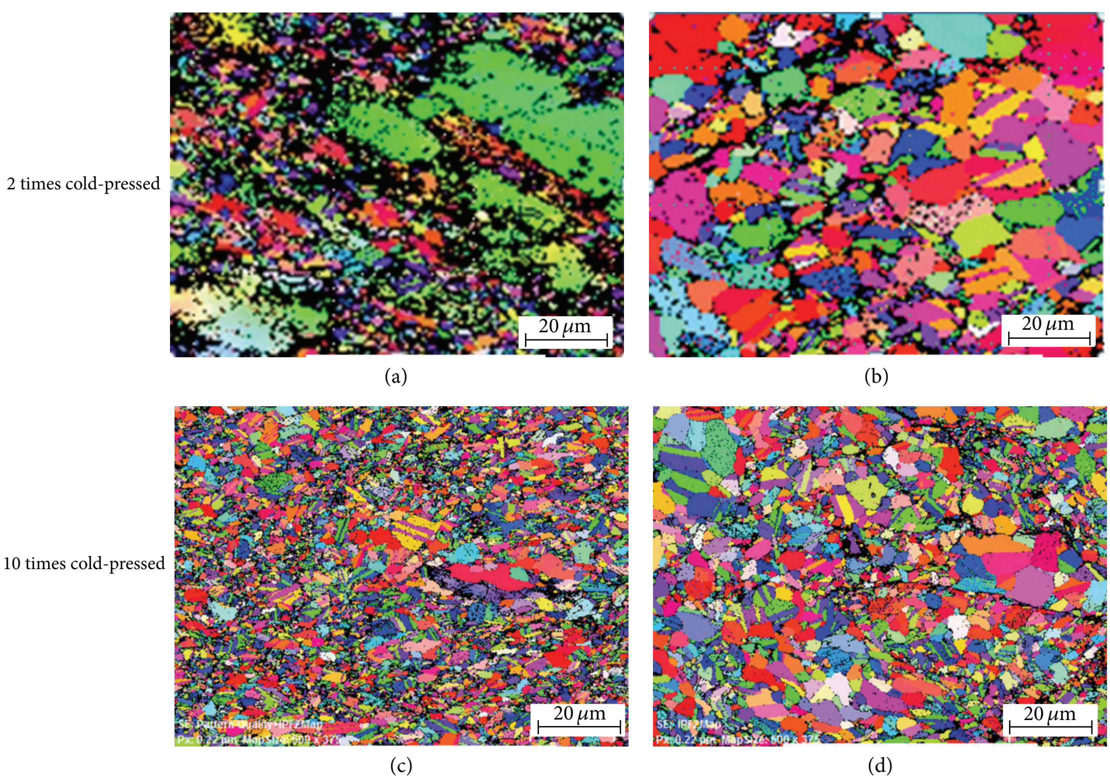

Figure 3: Electron Back-Scatter Diffraction (EBSD) images of $(Bi_{0.225}Sb_{0.775})_2Te_3$ alloys versus annealing time at 573 K with different number of cold-pressing. 2 times cold-pressed and annealed for (a) 2 hrs, (b) 30 hrs, 10 times cold-pressed and annealed for (c) 2 hrs, and (d) 30 hrs.

of cold-pressing and annealing time was carried out. Figure 3 illustrates an EBSD image of the samples which were cold-pressed 2 and 10 times followed by annealing for 2 and 30 hrs, respectively. It is clear that the more repetition of pressing process of the sample, the smaller the grain can be found. Dark areas in Figures 3(a) and 3(b) are due to the lattice distortions, such as dislocations and vacancies. The image in Figure 3(a) exhibits unclear grain structure and further annealing leads to grain structure with the size of a few tens of micrometers (Figure 3(b)). The decrease of the dark areas especially inside the 2 times cold-pressed grains means the recovery happened during the annealing process. However, it is easily recognized from Figures 3(c) and 3(d) that the annealing led to dynamic recrystallization and significant

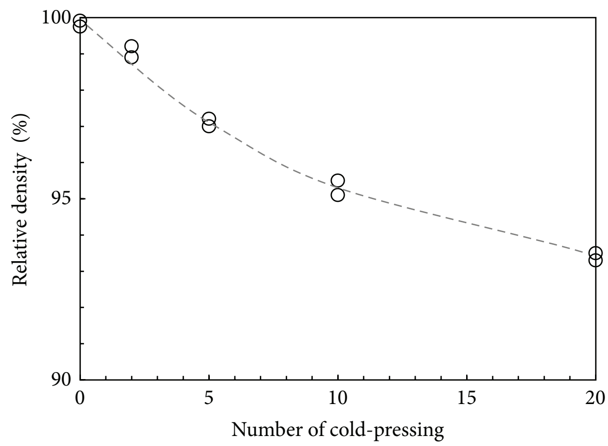

FIGURE 4: Change of relative density for $(Bi_{0.225}Sb_{0.775})_2Te_3$ alloys with the number of cold-pressing.

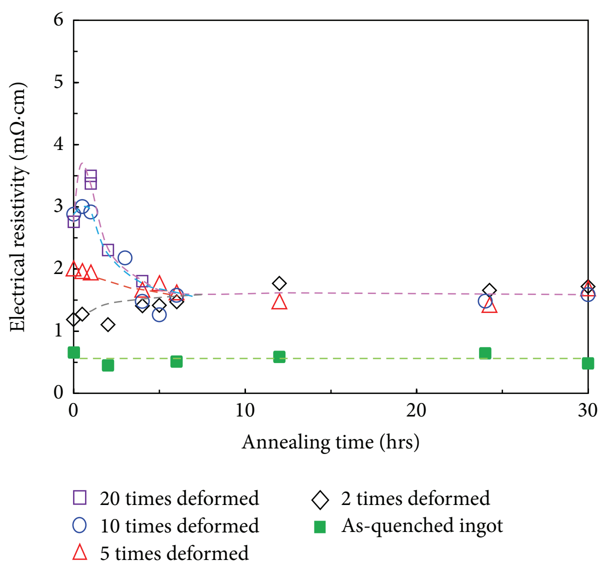

FIGURE 5: Change of the electrical resistivity of $(Bi_{0.225}Sb_{0.775})_2Te_3$ alloys with the number of cold-pressing and annealing time at 573 K.

increase of grain size for the 10 times cold-pressed samples. The change of the microstructure during annealing may cause changes in thermoelectric properties such as resistivity and Seebeck coefficient.

The relative density of the samples with the number of cold-pressing is shown in Figure 4, and the electrical resistivity with different annealing time is shown in Figure 5. Initially, a pronounced electrical resistivity increase is observed in the highly deformed samples. Heat treatment process produces a strong decrease of electrical resistivity especially for highly deformed sample and the values were saturated after 6 hrs of heat treatment. The relative density values were decreased with an increase of the number of cold-pressing process. The annealing of the specimen does not lead to densification in the whole observed region.

In general, when a metal is deformed below its recrystallization temperature, it is said to be "cold-worked." All

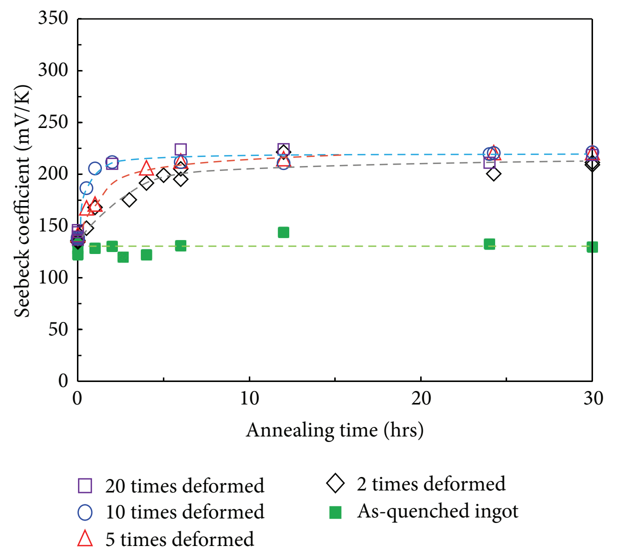

FIGURE 6: Change of the Seebeck coefficient of $(Bi_{0.225}Sb_{0.775})_2Te_3$ alloys with the number of cold-pressing and annealing time at 573 K.

the properties of a metal that are dependent on the lattice structure are affected by plastic deformation or cold-working [14, 15]. Cold-pressing process in this work produces very high deformation enough to fracture the ingot into fine particles. This is related to relatively low ductility and mechanical strength of the Bi-Te-based alloy compared to a metal and the presence of cleavage planes. The decrease of relative density in Figure 4 may be attributed to the increase of fine particles with cold-working since large grains have broken into smaller pieces and as they are smaller their porosity constantly increases.

The electrical resistivity in polycrystalline structures can depend on a grain size, porosity, carrier density, and its mobility [16, 17]. It is well known that the electrical resistivity is determined competitively by carrier concentration and mobility as described by the relationship: $\rho = 1/ne\mu$, where n, μ, and e are the carrier concentration, carrier mobility, and electron charge, respectively. The decrease of electrical resistivity with annealing time, especially in highly deformed samples (10 and 20 times cold-pressed samples in Figure 5, can be explained by an increased electrical mobility because of the grain growth during the annealing process. This would be associated with a decrease in total scattering of charge carriers and annihilation of deformed stress in the sample, leading to enhanced conductivity.

Figure 6 shows the Seebeck coefficient of cold-pressed samples as a function of annealing time. The positive values of Seebeck coefficient indicate that all the samples are p-type materials. All the as-deformed specimens showed the same Seebeck coefficient of about 140 μV/K. However, these values were increased with increase of annealing time. Interestingly, the Seebeck coefficient of the samples cold-pressed 10 and 20 times repetition were sharply increased in relatively short annealing periods of about 2 hrs, and saturated to the value of

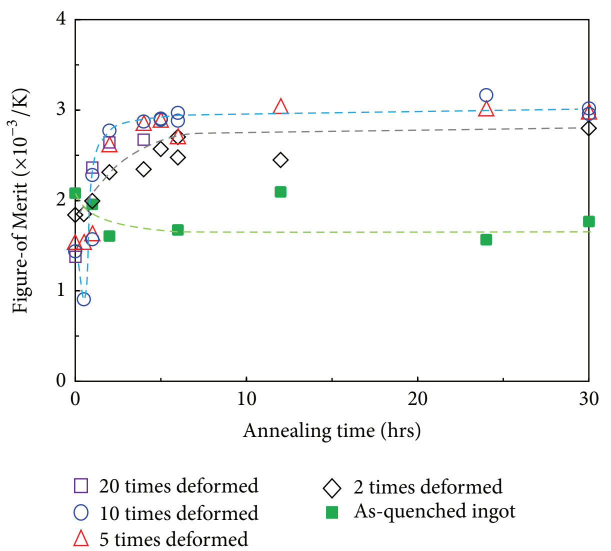

FIGURE 7: Change of the Figure-of-Merit of $(Bi_{0.225}Sb_{0.775})_2Te_3$ alloys with the number of cold-pressing and annealing time at 573 K.

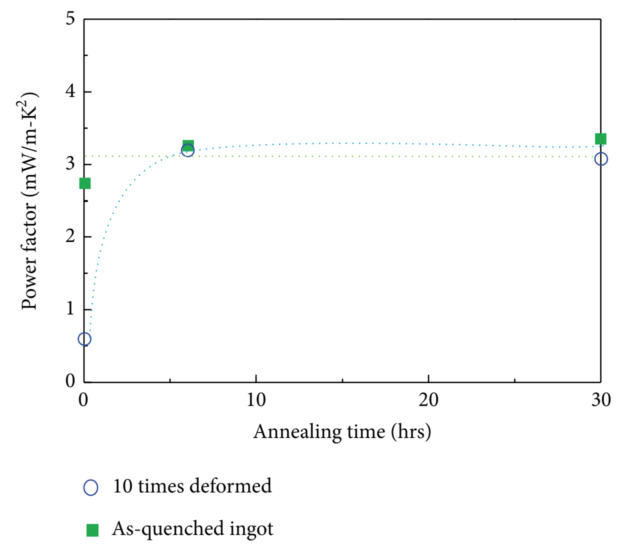

FIGURE 8: Change of the power factor of $(Bi_{0.225}Sb_{0.775})_2Te_3$ alloys of as-quenched ingot and the 10 times cold-pressing with annealing time at 573 K.

about 220 μV/K. The Seebeck coefficient of the samples cold-pressed 2 or 5 times repetition increased slowly compared to that of the samples cold-pressed 10 and 20 times.

It is well known that Seebeck coefficient is mostly governed by effective mass and carrier concentrations, and independent of the grain size. In highly deformed samples, it should be pointed out that large amount of dislocations, point defects, and antistructure defects may increase the electrical carriers with very low mobility, and these are responsible for high electrical resistivity. More detailed analysis on exact structure of generated defects according to cold-pressing and how these defects affect thermoelectric properties is beyond the scope of this paper. Accordingly, it is thought that the time needed for recrystallization of crushed particles in the cold-pressed Bi-Sb-Te compounds depend on the number of cold-pressing process. The enhancement of Seebeck coefficient with annealing can be considered by two aspects: the reduction of carrier concentration with annihilation of residual defects and recrystallization.

Room temperature Figure-of-Merit (Z) of the cold-pressed alloys as a function of annealing time are plotted in Figure 7, respectively. Z values are rapidly increased with annealing time especially in highly deformed alloy. The highest Figure-of-Merit of the sample reaches about 3.0×10^{-3}/K at 300 K, which is lower than the zone-melted one and that of state-of-art Bi_2Te_3-Sb_2Te_3-based materials [2, 18]. The power factors of as-quenched ingot and 10 times deformed sample are plotted as the function of the annealing time in Figure 8. As shown in the figure, the power factors of annealed ingot exhibited similar values to those in deformed samples after annealing. Even though the low Seebeck values are in as-quenched ingot, the low resistivity of the ingot resulted in similar values for power factors with highly deformed samples after annealing. Thus, the improvement of Z value in a highly deformed sample is mainly attributed to reduced thermal conductivity. During the annealing process, new grain structure with a submicron size is generated by the recrystallization and grain coarsening. Although the Z value is still low, the fabrication method of bulk Bi_2Te_3-based compounds introduced here is more cost effective. It is also much easier compared to other powder-base fabrication techniques for bulk thermoelectric materials and it can be easily scaled up for commercial applications.

4. Conclusions

The effects of the repetition of cold-pressings followed by recovery annealing on the thermoelectric properties were investigated for $(Bi_{0.225}Sb_{0.775})_2Te_3$ alloys. Generally, the plastic deformation increases dislocation density and changes grain size distribution in single and polycrystalline materials. In this experiment, the mechanical pressure of 700 MPa is high enough to fracture the as-quenched ingot into fine particles. Thus, high density of dislocation as well as the reduction of grain size may be expected in our cold-pressed samples. The grain size of cold-pressed samples was controlled by the number of cold-press processing and annealing times. The high electrical resistivity in highly deformed samples is mainly attributed to the increase of grain boundary scattering due to the reduction of grain size and high porosity. The enhancement of the Seebeck coefficient with annealing is mainly related to the recovery and recrystallization of the deformed samples. The recrystallization process can be obtained by diffusion process or annihilation of generated defect. The time needed for recrystallization with annealing depend on the grain size and porosity; the smaller the grain size, the shorter the diffusion distances. The fast saturation of Seebeck coefficient in highly deformed samples with annealing indicates that the Seebeck coefficient is independent of the grain size. However, further decrease in electrical resistivity was observed after Seebeck coefficient saturation. Increase in mobility could occur due to the grain growth which reduces the grain boundary scattering for electron transport.

It is worth mentioning that our cold-press processing does not employ any methods to prepare powder of the materials. Even we did not use powdering process; fine grained structure is obtained by simple repetition of cold-pressing followed by annealing. Accordingly, it seems reasonable to conclude that the improvement of thermoelectric performance in $(Bi_{0.225}Sb_{0.775})_2Te_3$ compound is possible by using cold-deformation and recovery annealing process. Investigations on optimization of composition and microstructural adjustment are required for further enhancement of ZT. Our approaches provide cost-effective fabrication method of Bi_2Te_3-based alloys with high thermoelectric performance.

Conflict of Interests

The authors declare that there is no conflict of interests regarding the publication of this paper.

Acknowledgment

This research was supported by the Converging Research Center Program through the Ministry of Education, Science and Technology (2013K000168).

References

[1] D. M. Rowe, *CRC Handbook of Thermoelectrics*, CRC, 1995.

[2] B. Poudel, Q. Hao, Y. Ma et al., "High-thermoelectric performance of nanostructured bismuth antimony telluride bulk alloys," *Science*, vol. 320, no. 5876, pp. 634–638, 2008.

[3] R. Venkatasubramanian, E. Siivola, T. Colpitts, and B. O'Quinn, "Thin-film thermoelectric devices with high room-temperature figures of merit," *Nature*, vol. 413, no. 6856, pp. 597–602, 2001.

[4] Y. Ma, Q. Hao, B. Poudel et al., "Enhanced thermoelectric figure-of-merit in p-type nanostructured bismuth antimony tellurium alloys made from elemental chunks," *Nano Letters*, vol. 8, no. 8, pp. 2580–2584, 2008.

[5] W. Xie, J. He, H. J. Kang et al., "Identifying the specific nanostructures responsible for the high thermoelectric performance of $(Bi,Sb)_2Te_3$ nanocomposites," *Nano Letters*, vol. 10, no. 9, pp. 3283–3289, 2010.

[6] G. Joshi, H. Lee, Y. Lan et al., "Enhanced thermoelectric figure-of-merit in nanostructured p-type silicon germanium bulk alloys," *Nano Letters*, vol. 8, no. 12, pp. 4670–4674, 2008.

[7] Y. Q. Cao, X. B. Zhao, T. J. Zhu, X. B. Zhang, and J. P. Tu, "Syntheses and thermoelectric properties of Bi_2Te_3/Sb_2Te_3 bulk nanocomposites with laminated nanostructure," *Applied Physics Letters*, vol. 92, no. 14, Article ID 143106, 2008.

[8] Y. Zhao, J. S. Dyck, B. M. Hernandez, and C. Burda, "Enhancing thermoelectric performance of ternary nanocrystals through adjusting carrier concentration," *Journal of the American Chemical Society*, vol. 132, no. 14, pp. 4982–4983, 2010.

[9] X. Tang, W. Xie, H. Li, W. Zhao, Q. Zhang, and M. Niino, "Preparation and thermoelectric transport properties of high-performance *p*-type Bi_2Te_3 with layered nanostructure," *Applied Physics Letters*, vol. 90, no. 1, Article ID 012102, 2007.

[10] D.-B. Hyun, J.-S. Hwang, J.-D. Shim, and T. S. Oh, "Thermoelectric properties of $(Bi_{0.25}Sb_{0.75})_2Te_3$ alloys fabricated by hot-pressing method," *Journal of Materials Science*, vol. 36, no. 5, pp. 1285–1291, 2001.

[11] S. Miura, Y. Sato, K. Fukuda, K. Nishimura, and K. Ikeda, "Texture and thermoelectric properties of hot-extruded Bi_2Te_3 compound," *Materials Science and Engineering A*, vol. 277, no. 1-2, pp. 244–249, 2000.

[12] S. S. Kim, S. Yamamoto, and T. Aizawa, "Thermoelectric properties of anisotropy-controlled *p*-type Bi-Te-Sb system via bulk mechanical alloying and shear extrusion," *Journal of Alloys and Compounds*, vol. 375, no. 1-2, pp. 107–113, 2004.

[13] J.] Jiang, L. Chen, S. Bai, Q. Yao, and Q. Wang, "Fabrication and thermoelectric performance of textured n-type $Bi_2(Te, Se)_3$ by spark plasma sintering," *Materials Science and Engineering B*, vol. 117, no. 3, pp. 334–338, 2005.

[14] C. S. Çetinarslan, "Effect of cold plastic deformation on electrical conductivity of various materials," *Materials and Design*, vol. 30, no. 3, pp. 671–673, 2009.

[15] Z.-C. Chen, K. Suzuki, S. Miura, K. Nishimura, and K. Ikeda, "Microstructural features and deformation-induced lattice defects in hot-extruded Bi_2Te3 thermoelectric compound," *Materials Science and Engineering A*, vol. 500, no. 1-2, pp. 70–78, 2009.

[16] J. Jaklovszky, R. Ionescu, N. Nistor, and A. Chiculita, "Grain size effect on the figure of merit of sintered solid solutions based on Bi_2Te_3," *Physica Status Solidi*, vol. 27, no. 2, pp. 329–332, 1975.

[17] A. Kumar, D. Singh, and D. Kaur, "Grain size effect on structural, electrical and mechanical properties of NiTi thin films deposited by magnetron co-sputtering," *Surface and Coatings Technology*, vol. 203, no. 12, pp. 1596–1603, 2009.

[18] T. M. Tritt, "Holey and unholey semiconductors," *Science*, vol. 283, no. 5403, pp. 804–805, 1999.

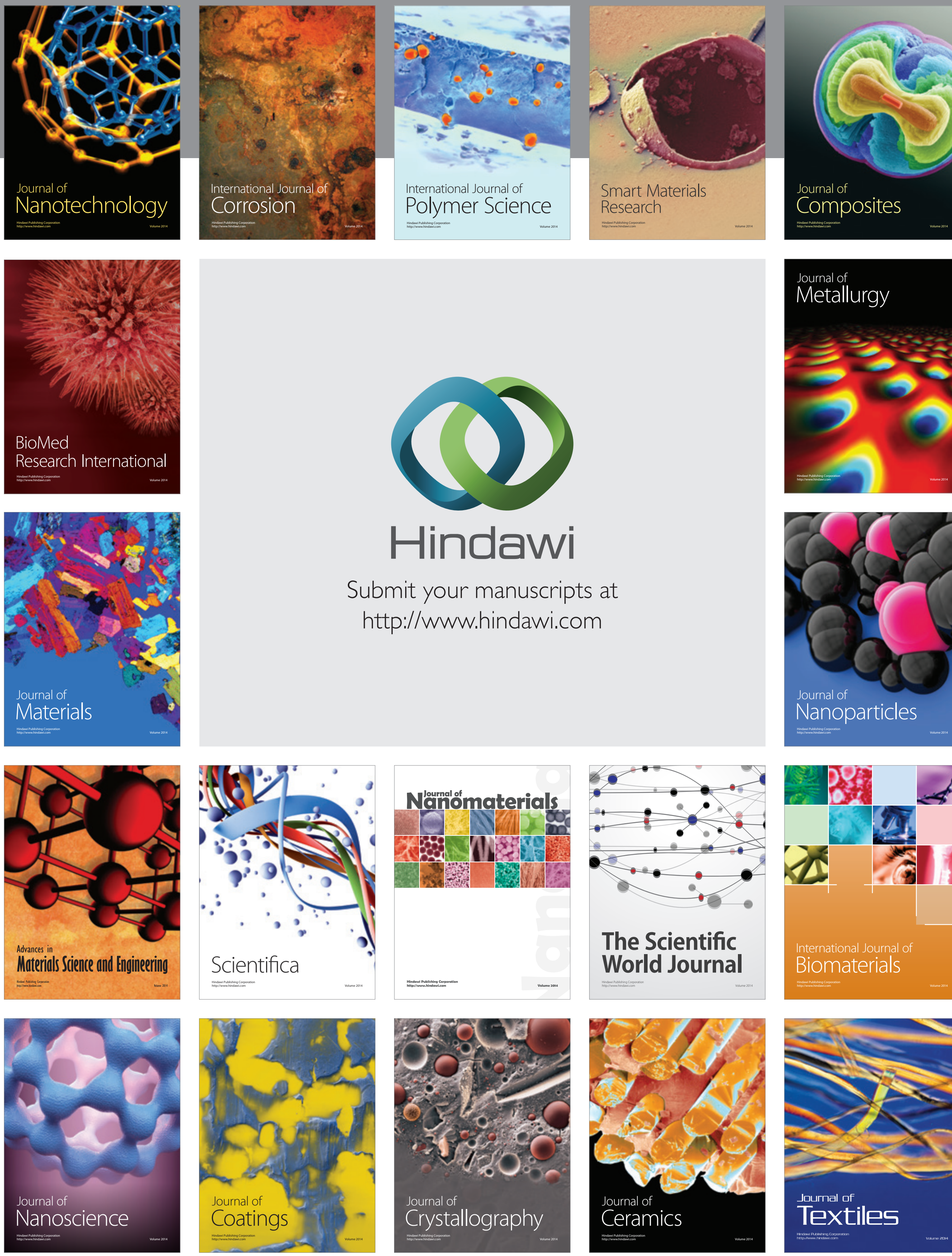
Journal of
Nanotechnology
International Journal of
Corrosion
International Journal of
Polymer Science
Smart Materials
Research
Journal of
Composites
BioMed
Research International
Hindawi
Submit your manuscripts at
http://www.hindawi.com
Journal of
Metallurgy
Journal of
Materials
Journal of
Nanoparticles
Advances in
Materials Science and Engineering
Scientifica
Journal of
Nanomaterials
The Scientific
World Journal
International Journal of
Biomaterials
Journal of
Nanoscience
Journal of
Coatings
Journal of
Crystallography
Journal of
Ceramics
Journal of
Textiles